GEOPIER FOUNDATION CO INC
TECHNICAL BULLETIN

No. 2

BEARING CAPACITY OF GEOPIER-SUPPORTED FOUNDATION SYSTEMS

This Technical Bulletin discusses the bearing capacity of Geopier®-supported foundation elements. The behavior of both single Geopier elements and groups of Geopier elements is complex because of the changes in the stress state of the matrix soils as a result of ramming action during Geopier installations, and because of the complicated load-transfer mechanisms that occur between the loaded footing, the relatively stiff Geopier reinforcing elements, and the relatively soft matrix soil. Because of these complicated interactions, simplifying approaches and assumptions have been used within the analyses presented herein. Ultimate bearing pressures are computed using limit equilibrium theories of classical soil mechanics in conjunction with idealized failure geometries necessary to make the systems solvable. Limit equilibrium solutions are considered to be lower bound approximations compared with upper bound approximations derived from energy considerations. The solutions presented herein conservatively neglect the confining influence provided by the loaded footings and provided by adjacent Geopier elements.

1. LIMIT EQUILIBRIUM BEARING CAPACITY FAILURE MODES

The allowable bearing pressure for Geopier-supported footings is nearly always controlled by settlement considerations. It is possible, however, to apply sufficient bearing pressure so that the yield strength of the underlying Geopier-reinforced soil is reached. The bearing pressure associated with fully mobilized shear strength is defined as the limit equilibrium bearing capacity of the footing. Classical shearing surfaces are typically assumed to extend along circular and log-spiral surfaces below footings not supported by Geopier reinforcing elements (Figure 1). The potential for shearing within a Geopier-reinforced soil matrix is more difficult to determine, however, because of the complicated interactions between the strong Geopier elements and the relatively weak matrix soil. The potential limit equilibrium failure modes for Geopier-supported footings consist of:

1. Bulging failure of individual Geopier elements (Figure 2a, page 7),
2. Shearing below the tips of Geopier elements (Figure 2b, page 7),
3. Shearing within the Geopier-reinforced soil matrix (Figure 2c, page 7), and
4. Shearing below the bottom of the Geopier-reinforced soil matrix (Figure 2d, page 7).

The following Sections present design approaches used to estimate the bearing capacity associated with each of the failure modes described above. The developed expressions can be used to estimate the bearing capacity of Geopier-supported footings on a case-by-case basis. To provide generalized design guidance, tables of allowable footing bearing pressures for typical design conditions are presented herein for each mode of potential failure. Typical design conditions are presented in Table 1. The results of the analyses presented herein for typical design conditions indicate that shearing below the bottoms of individual Geopier elements (Figure 2b) and within the Geopier-reinforced soil matrix (Figure 2c) often controls the bearing capacity design.

Figure 1.
Limit Equilibrium Bearing Capacity of Conventional Spread Footings.

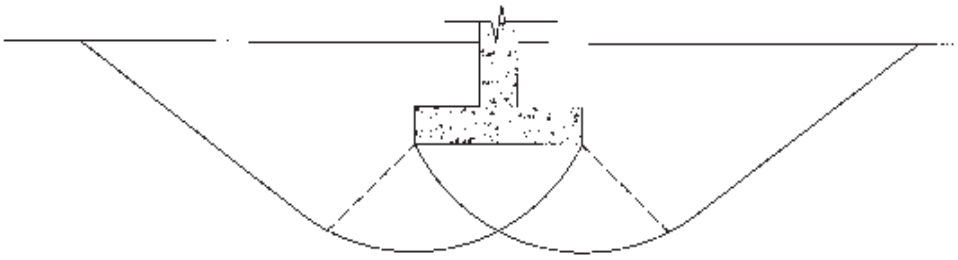

2. BULGING FAILURE OF INDIVIDUAL GEOPIER ELEMENTS

The potential for the bulging failure of individual granular columnar elements in saturated clays is described by Mitchell (1981) and depicted in Figure 2a. If sufficient pressure is applied to the tops of Geopier elements, the shear strength could be fully mobilized within the elements and along surfaces extending through the surrounding soil matrix. The development of shearing surfaces within the Geopier elements cause the Geopier elements to bulge outward. The lateral earth pressure in the matrix soils around the Geopier elements resists outward bulging. Because lateral earth pressures are lowest near the ground surface where overburden stresses are low, the greatest amount of bulging occurs in the upper portions of the Geopier elements.

Hughes and Withers (1974) used cavity expansion theory to formulate an expression for the bearing capacity of single granular columnar elements subject to bulging deflections. For Geopier elements installed in cohesive soil, the ultimate stress that may be applied to the top of the Geopier element ($q_{ult,g}$) may be estimated by the product of the limiting radial stress and the Rankine passive earth pressure coefficient of the Geopier aggregate material:

$$q_{ult,g} = \sigma_{r,lim} \tan^2 (45 + \phi_g/2), \qquad Eq.1.$$

where ϕ_g is the friction angle of the Geopier aggregate material. The limiting radial stress may be estimated

using the following expression:

$$\sigma_{r,lim} = \sigma_{r,o} + c\ \{1 + \ln [E/(2\ c(1 + \mu))]\}, \quad Eq.2.$$

where $\sigma_{r,o}$ is the total radial stress after the installation of the Geopier element and prior to the application of the footing load, c is the undrained shear strength of the matrix soil, E is the undrained modulus of the matrix soil, and μ is Poisson's ratio of the matrix soil. The total radial stress after the installation of the Geopier element is the sum of the effective radial stress and the pore water pressure. The results of Geopier uplift load tests and the results of in-situ measurements taken with the Stepped Blade and the Menard Pressuremeter after Geopier installations indicate that the effective horizontal pressure in the matrix soil after Geopier installation may be estimated as the product of the effective vertical stress and the Rankine passive earth pressure coefficient ($k_{p,s}$) of the matrix soil. Assuming an effective stress friction angle of 20 degrees for saturated clay and neglecting the additive influence of pore water pressure, the total radial stress after the installation of the Geopier element is about twice as large as the effective vertical overburden stress. Because the ratio of the undrained modulus (E) to the undrained shear strength (c) of the clay may be conservatively estimated to be about 200 and because Poisson's ratio for undrained conditions is 0.5, Equation 2 may be simplified as:

$$\sigma_{r,lim} = 2\sigma_v' + 5.2\ c. \quad Eq.3.$$

Combining Equation 1 and Equation 3, and incorporating a Geopier friction angle of 50 degrees, which is substantiated from the results of full-scale direct shear tests performed for Geopier elements, the ultimate bearing capacity of a single Geopier element may be estimated as:

$$q_{ult,g} = 15.1\ \sigma_v' + 39.3\ c. \quad Eq.4.$$

The vertical effective stress should be estimated as the average overburden stress at the depth within the soil matrix corresponding to Geopier bulging. The portion of the Geopier element that is most likely to fail by bulging extends from the bottom of the footing to a depth equal to the product [d tan(45+ϕ_g/2)] below the bottom of the footing, where d is the Geopier diameter. For a 30-inch diameter Geopier element installed 2 feet below adjacent grade, the depth to the middle of the critical bulging zone is 5.4 feet. Combining this depth with the typical design values presented in Table 1, Equation 4 may be further simplified as:

$$q_{ult,g} = 6{,}580\ psf + 39.3\ c. \quad Eq.5.$$

Table 2 presents calculated values of allowable top-of-Geopier pressure and allowable footing bearing pressure. The relationship between top-of-Geopier stress and average footing bearing stress is described in Table 1.

The calculations presented above are considered to be conservative because they do not include vertical confining stresses provided by the overlying loaded footing and because of the implementation of Rankine earth pressure conditions that do not account for additional normal and shear stresses associated with the construction of the Geopier elements. The additional normal and shear stresses that result from Geopier installations rotate the principal stresses, thus allowing for horizontal stresses in excess of those computed using the Rankine expression.

3. SHEARING BELOW THE TIPS OF INDIVIDUAL GEOPIER ELEMENTS

The potential for shearing below the bottom of individual Geopier elements is depicted in Figure 2b. Neglecting the weight of the pier material, the total load applied to the tops of Geopier elements ($Q_{top,g}$) is resisted by both shaft friction (Q_{shaft}) and end-bearing of the Geopier tip ($Q_{tip,g}$):

$$Q_{top,g} = Q_{shaft} + Q_{tip,g}, \qquad Eq.6.$$

which can be rewritten in terms of stress as:

$$q_{ult,g}A_g = f_sA_{shaft} + q_{tip,g}A_g, \qquad Eq.7.$$

where $q_{ult,g}$ is the ultimate stress applied at the top of the Geopier element, A_g is the cross-sectional area of the Geopier element, f_s is the average unit friction along the Geopier shaft, A_{shaft} is the area of the Geopier shaft, and $Q_{tip,g}$ is the stress resisted at the tip of the Geopier element. Rearranging Equation 7, the ultimate top-of-Geopier stress may be expressed as:

$$q_{ult,g} = f_sA_{shaft}/A_g + q_{tip,g} = 4f_sd_{shaft}H_{shaft}/d^2 + q_{tip,g}, \qquad Eq.8.$$

where d_{shaft} is the diameter of the Geopier shaft, d is the nominal diameter of the Geopier element, and H_{shaft} is the length of the Geopier shaft. The parameters d_{shaft} and d are described separately because the effective radius of the Geopier shaft is estimated to be approximately 3 inches greater than the nominal shaft radius as a result of ramming the aggregate stone laterally during densification with the beveled Geopier tamper.

The bearing capacity of the tip of the Geopier element may be estimated with the classical Terzaghi-Buisman equation:

$$q_{tip,g} = q_{ult} = c\,N_c + 0.5\,d_{shaft}\,\gamma\,N_\gamma + \sigma_v'\,N_q, \qquad Eq.9.$$

where N_c, N_γ, and N_q are dimensionless bearing capacity factors, γ is the matrix soil unit weight, and σ_v' is the overburden stress at the elevation of the tip of the Geopier element.

UNDRAINED CONDITIONS

For undrained conditions, the average unit friction along the Geopier shaft (f_s) is the average undrained shear strength (c) of the matrix soil in the vicinity of the Geopier shaft. The expression for tip bearing capacity (Equation 9) in clay soils may be simplified to (Meyerhof 1976):

$$q_{tip} = c\,N_c. \qquad Eq.10.$$

Experience with driven and bored piles indicates that N_c in undrained clay is approximately 9. Equation 8 then becomes:

$$q_{ult,g} = 4c\,d_{shaft}H_{shaft}/d^2 + 9c. \qquad Eq.11.$$

The consequence of excessive normal stress at the tips of the Geopier elements is settlement, not global footing rotation. This is because footing stresses will be transferred to the matrix soil materials as the Geopier shafts

settle more than anticipated. Although safety factors are not normally considered in geotechnical settlement calculations, a factor of safety of 1.5 is considered to be prudent for this potential mode of Geopier deflection. Table 3 presents calculated values of allowable top-of-Geopier pressure and allowable footing bearing pressure for the typical design values described in Table 1. To provide for a safe design, a factor of safety of 1.5 is implemented in the calculations.

The calculations presented above are considered to be conservative because they do not include the effects of matrix soil strength gain as a result of Geopier installation, and they account for only three inches of radial expansion during Geopier installation. These assumptions are considered to be particularly conservative for short Geopier elements installed in very soft soil conditions. Additionally, the calculations presented above are applicable only to soils for which the rate of excess pore water pressure dissipation is slower than the rate of loading. For these reasons it is recommended that the design of single Geopier elements installed in very soft clays be based on the results of a Geopier load test.

DRAINED CONDITIONS

For drained conditions, the average unit friction along the Geopier shaft (f_s) is the product of the average effective horizontal pressure (σ_h') and the tangent of the friction angle of the matrix soil [$\tan(\phi_s)$]. The average effective horizontal pressure may be conservatively estimated as the product of the effective vertical stress acting at the midpoint of the shaft length ($\sigma_{v'avg}$) and the Rankine passive earth pressure coefficicient ($k_{p,s}$) of the matrix soil. The average unit friction may therefore be expressed as:

$$f_s = \sigma_{v'avg} \tan(\phi_s)\, k_{p,s} = (d_f + H_{shaft}/2)\, \gamma \tan(\phi_s) \tan^2(45 + \phi_s/2), \quad \textit{Eq.12.}$$

where d_f is the depth of the bottom of the footing below adjacent grade, H_{shaft} is the Geopier shaft length below the bottom of the footing, γ is the buoyant unit weight of the matrix soil, and ϕ_s is the friction angle of the matrix soil. The bearing capacity of the tip of the Geopier element may be estimated with Equation 9, above, where the first term is omitted because c is taken to be zero and where the second term is negligible for shallow Geopier elements. The bearing capacity factor N_q depends on the friction angle of the soil. Matrix soil friction angles of 20, 25, 27, 30, and 35 degrees are associated with N_q values of 10, 20, 30, 40, and 90, respectively (Meyerhof 1976).

As noted above, a safety factor of 1.5 is considered to be prudent for the calculations because the consequence of excessive normal stress at the tips of the Geopier elements is settlement, not global footing rotation. Table 4 presents calculated values of allowable top-of-Geopier pressure and allowable footing bearing pressure for the typical design values described in Table 1. The calculations implement a factor of safety of 1.5 to provide for a safe design for the limitation of excessive Geopier settlement.

The calculations presented above are considered to be conservative because they do not include vertical confining stresses provided by the overlying loaded footing and they account for only three inches of radial expansion during Geopier installation. These assumptions are considered to be particularly conservative for short Geopier elements installed in very soft or loose soil conditions. For these reasons, it is recommended that the design of single Geopier elements installed in soft or loose materials be based on the results of a Geopier load test.

4. SHEARING WITHIN THE GEOPIER-REINFORCED SOIL MATRIX

The potential for shearing within the Geopier-reinforced soil matrix is depicted in Figure 2c. For this failure mode, shear planes are assumed to pass through the Geopier elements and matrix soils and then upward through the surrounding soils. The shear strength of the materials along the assumed failure plane depends on the frictional resistance to shearing within the matrix soil (t_s) and the frictional resistance to shearing offered by the Geopier elements (t_g). Mitchell (1981) summarizes approaches formulated by Priebe (1978) and Aboshi et al. (1979) that use composite shear strength parameters to provide solutions for this condition. Once composite shear strength parameters are developed, the bearing capacity of the composite soil matrix may be estimated using the conventional Terzaghi-Buisman bearing capacity equation (Equation 9). Priebe (1978) recommends that the composite friction angle of the reinforced soil (ϕ_{comp}) and composite cohesion intercept (c_{comp}) be estimated with the expressions:

$$\phi_{comp} = \tan^{-1} [R_a\, n \tan(\phi_g) + (1-R_a\, n) \tan(\phi_s)] \quad \textit{Eq.13}.$$

and

$$c_{comp} = (1-R_a\, n)\, c, \quad \textit{Eq.14}.$$

where R_a is the ratio of the area coverage of the Geopier elements to the gross area of the soil matrix in the area of shearing, n is the ratio of the stress applied to the Geopier elements to the stress applied to the matrix soil, ϕ_g is the friction angle of the Geopier elements, ϕ_s is the friction angle of the matrix soil, and c is the cohesion intercept of the matrix soil. Aboshi et al. (1979) provide a similar solution but recommend that the shear strength of the columnar element be modified by the cosine of the angle of the intercepting shear plane with respect to horizontal. This is to account for differences between the vertical stress acting on vertical planes within the columnar element and the normal stress acting on the shear plane.

The Priebe and Aboshi approaches may be implemented by using the expressions shown in Equations 13 and 14 above, provided that the effects of Geopier and failure plane geometry and the effects of Geopier stress reductions with depth are considered. To account for shearing planes that extend beyond the footprint of the concrete foundation, it is recommended that R_a be estimated by modifying the Geopier/footing coverage area ratio (typically about 0.33) by a reduction factor of 0.4. This reduction factor results in an effective R_a value of about 0.13 for typical design conditions.

The stress ratio value (n) should be selected to reflect the distribution of stresses at the location of the shearing plane. At the tops of the Geopier elements, the stress concentration factor is often about 12. Vertical stresses in the Geopier elements decrease with depth, however, as loads are transferred to the surrounding matrix soil. Aboshi et al. (1979) recommend that the normal stress reductions with depth within the granular columnar elements be estimated using elastic solutions. It is therefore recommended that the stress concentration factor be estimated by reducing the stress concentration at the bottom of the footing by a factor representing a 2:1 (vertical to horizontal) rate of load spreading below the footing.

The shear strength of the composite soil changes with depth because it depends on the effects of load spreading and the orientation of the failure plane. A conservative solution may be achieved, however, by considering the composite shear strength at a depth of three-quarters of the footing width below the footing bottom and on a failure plane inclined 45 degrees from horizontal. The implementation of these conditions results in a soil matrix stress concentration factor of 2.8, which accounts for both depth and shear plane orientation considerations.

Table 5 presents calculated values of allowable footing bearing pressure for the typical design parameter values described in Table 1 and a soil matrix stress concentration factor of 2.8. It should be noted that even with conservatively selected parameter values, the results of the analysis presented in Table 5 indicate that this mechanism of potential failure only controls the design of footings constructed within strong matrix soils and provides for footing allowable bearing pressures that typically exceed design values. For these reasons, further refinement in the analysis does not appear to be warranted.

Figure 2. Potential Modes of Failure.

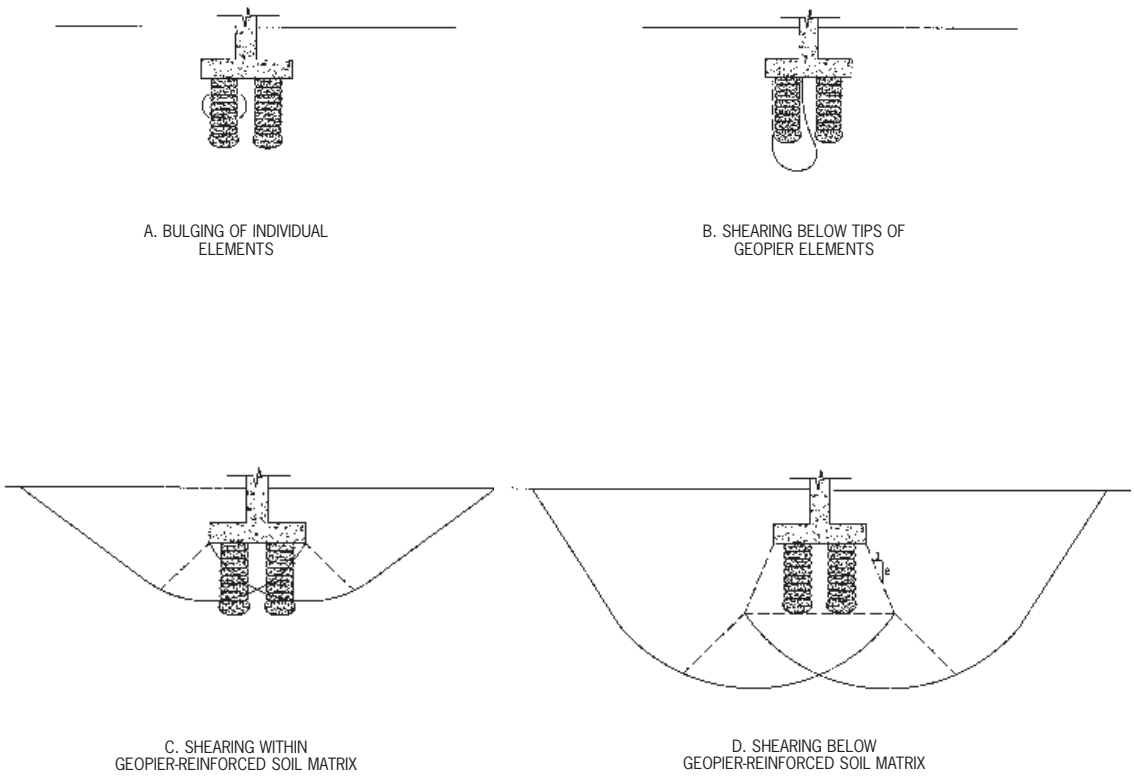

5. SHEARING BELOW THE BOTTOM OF THE GEOPIER-REINFORCED SOIL MATRIX

The potential for shearing below the bottom of the Geopier-reinforced soil matrix is depicted in Figure 2d. A conservative solution for this problem may be achieved by comparing the stresses induced at the bottom of the Geopier-enhanced soil layer with the allowable bearing pressure computed using Equation 9, above (NAVFAC 1983). The stress induced at the bottom of the Geopier-enhanced layer (q_{bottom}) may be estimated by assuming that load spreading increases at a rate of 2:1 (vertical to horizontal) below the bottom of the footing:

$$q_{bottom} = q \{BL/[(B + H)(L + H)]\}, \qquad Eq.15.$$

where q is the footing ultimate bearing pressure, B is the footing width, L is the footing length, and H is the thickness of the Geopier-enhanced soil layer. The ultimate footing bearing pressure may be estimated by computing the ultimate bearing pressure at the bottom of the reinforced soil matrix and multiplying this value by the inverse of the ratio shown in parentheses in Equation 15.

Tables 6 and 7 present calculated values of allowable footing bearing pressure for the typical design parameter values described in Table 1.

6. CONTROLLING BEARING CAPACITY

A comparison of the allowable footing bearing pressures for typical footings as presented in Tables 2 through 7 shows limit equilibrium bearing capacity within weak soils is typically controlled by the potential for shearing below the tips of individual Geopier elements. Limit equilibrium bearing capacity within strong soils is typically controlled by the potential for shearing within the Geopier-reinforced soil matrix. The controlling limit equilibrium bearing capacity for the typical conditions described in Table 1 and for all four modes of potential shearing is plotted on Figures 3 and 4 for undrained and drained conditions, respectively. The undrained chart (Figure 3) should be used only in situations in which the rate of loading is faster than the rate of footing load-induced matrix soil pore water pressure dissipation. The chart solutions are considered to be conservative, especially for relatively short Geopier elements installed in soft or loose soil materials. For this reason, it is recommended that Geopier bearing capacity in soft or loose soil conditions be estimated by the results of Geopier load tests.

Figure 3.
Footing Allowable Bearing Capacity for
Undrained Shearing and
Typical Design Conditions.

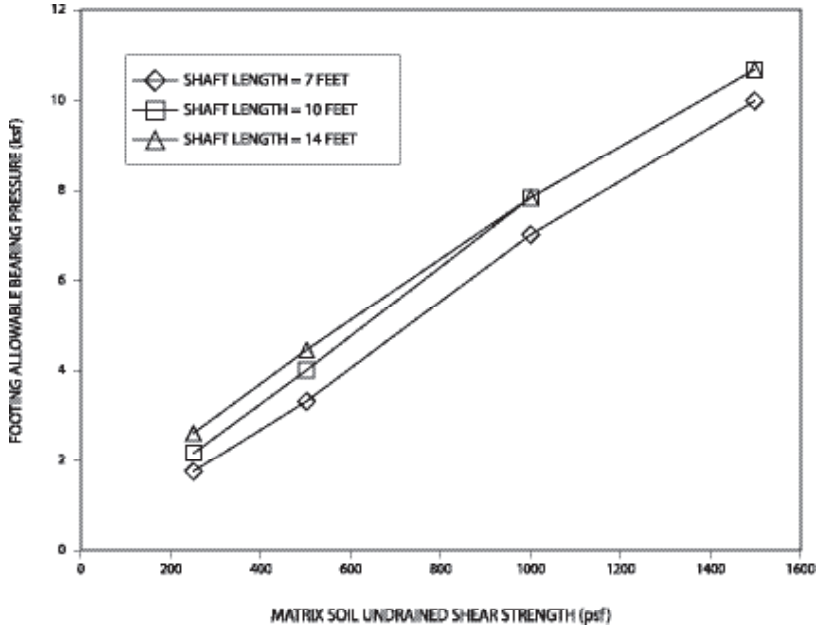

Figure 4.
Footing Allowable Bearing Capacity for
Drained Shearing and
Typical Design Conditions.

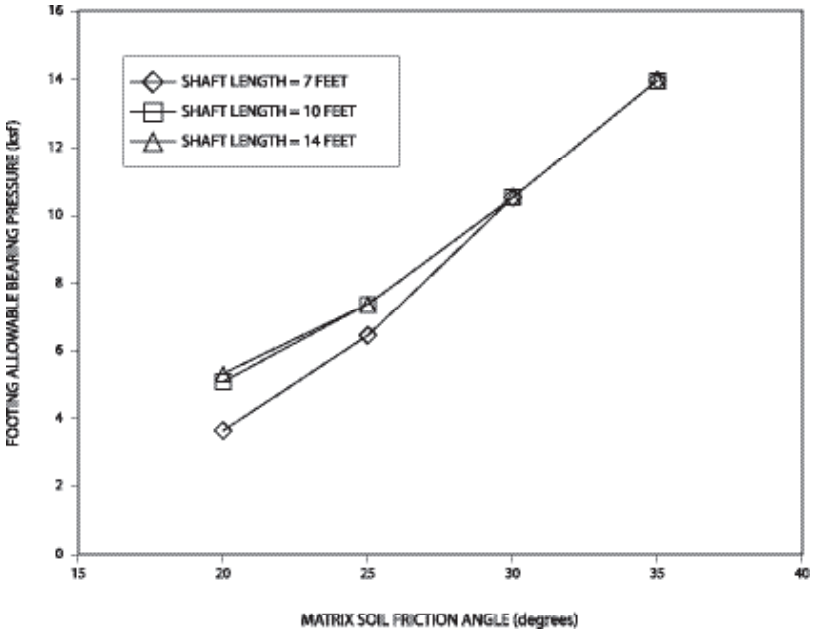

Table 1: Typical Geopier Design Conditions

PARAMETER	VALUE
Matrix soil total unit weight, γ_t	120 pcf
Depth to groundwater from ground surface	2 feet
Depth to footing bottom, d_f	2 feet
Nominal Geopier diameter, d	2.5 feet
Geopier shaft diameter after tamping, d_{shaft}	3 feet
Effective Geopier element shaft length	Drill length + 2 feet[1]
Geopier area replacement ratio (R_a)	0.33
Ratio of Geopier element to matrix soil stiffness moduli (R_s)[2]	12
Ratio of top-of-Geopier stress to average footing stress[3]	2.59
Geopier element friction angle, ϕ_g	50 degrees[4]
Factor of Safety	2.0[5]

Notes:

[1] A 2-foot addition to the Geopier drill length is incorporated in the analysis to incorporate the effects of the creation of a bottom bulb during construction and the effects of prestressing the bottom bulb soils during installation by ramming.

[2] Based on typical results from Geopier modulus load tests.

[3] Ratio of top-of-Geopier stress to average footing stress = $R_s/(R_sR_a - R_a + 1)$.

[4] Based on results of full-scale Geopier direct shear testing.

[5] Applicable for Geopier installations at project sites that include a Geopier load test. A factor of safety of 1.5 is applicable for shearing below the tips of individual Geopier elements because this mode of failure results in additional footing settlement rather than footing global rotation.

Table 2: Bearing Capacity Based on Bulging of Single Geopier Elements

MATRIX SOIL UNDRAINED SHEAR STRENGTH, c (psf)	ULTIMATE TOP-OF-GEOPIER STRESS (ksf)	ALLOWABLE TOP-OF-GEOPIER STRESS (ksf)	ALLOWABLE FOOTING BEARING PRESSURE (ksf)
250	16.4	8.2	3.2
500	26.2	13.1	5.1
750	36.0	18.0	6.9
1000	45.8	22.9	8.9
1500	65.5	32.7	12.6

Table 3: Bearing Capacity Based on Undrained Shearing Below Tips of Individual Elements

MATRIX SOIL UNDRAINED SHEAR STRENGTH, c (psf)	NOMINAL GEOPIER SHAFT LENGTH (ft)	ULTIMATE TOP-OF-GEOPIER STRESS (ksf)	ALLOWABLE TOP-OF-GEOPIER STRESS (ksf)	ALLOWABLE FOOTING BEARING PRESSURE (ksf)
250	7, 10, 14	6.1, 8.0, 9.9	4.4, 5.3, 6.6	1.7, 2.1, 2.6
500	7, 10, 14	12.2, 16.0, 19.9	8.8, 10.7, 13.2	3.4, 4.1, 5.1
1000	7, 10, 14	24.4, 32.0, 39.7	17.5, 21.4, 26.5	6.8, 8.2, 10.2
1500	7, 10, 14	36.5, 48.1, 59.6	26.3, 32.0, 39.7	10.1, 12.4, 15.3

Table 4: Bearing Capacity Based on Drained Shearing Below Tips of Individual Elements

MATRIX SOIL FRICTION ANGLE, ϕ_s (degrees)	NOMINAL GEOPIER SHAFT LENGTH (ft)	ULTIMATE TOP-OF-GEOPIER STRESS (ksf)	ALLOWABLE TOP-OF-GEOPIER STRESS (ksf)	ALLOWABLE FOOTING BEARING PRESSURE (ksf)
20 (clay)	7, 10, 14	12.4, 19.3, 27.6	9.3, 12.9, 18.4	3.6, 5.0, 7.1
25 (clay)	7, 10, 14	22.3, 34.1, 48.0	16.7, 22.8, 32.0	6.5, 8.8, 12.3
27 (silt)	7, 10, 14	30.8, 46.2, 64.1	23.0, 30.8, 42.7	8.9, 11.9, 16.5
30 (silt, silty sand)	7, 10, 14	40.5, 60.6, 83.8	30.2, 40.4, 55.8	11.7, 15.6, 21.6
35 (sand)	7, 10, 14	81.7, 119, 160	60.4, 79.1, 107	23.3, 30.5, 41.2

Table 5: Bearing Capacity Based on Failure Within Geopier-Reinforced Soil Matrix

MATRIX SOIL FRICTION ANGLE, ϕ_s (degrees)	MATRIX SOIL COHESION INTERCEPT, c (psf)	FOOTING WIDTH (ft)	ALLOWABLE FOOTING BEARING PRESSURE (ksf)
0 (clay)	250, 500, 1000	3	3.1, 4.6, 7.7
	250, 500, 1000	10	4.1, 5.6, 8.7
20 (clay)	0	3, 6, 10	5.3, 7.0, 9.4
25 (clay)	0	3, 6, 10	7.4, 10.0, 13.5
27 (silt)	0	3, 6, 10	8.5, 11.6, 15.7
30 (sandy silt, silty sand)	0	3, 6, 10	10.7, 14.6, 19.9
35 (sand)	0	3, 6, 10	13.9, 19.4, 26.6

Table 6: Bearing Capacity Based on Undrained Failure as a Group Below Soil Matrix

MATRIX SOIL COHESION INTERCEPT, c (psf)	FOOTING WIDTH (ft)	GEOPIER SHAFT LENGTH (ft)	ALLOWABLE FOOTING BEARING PRESSURE (ksf)
250	6	7, 10, 14	4.0, 5.8, 8.6
	10	7, 10, 14	2.3, 3.1, 4.3
500	6	7, 10, 14	8.0, 11.6, 17.3
	10	7, 10, 14	4.6, 6.2, 8.7
1000	6	7, 10, 14	16.0, 23.1, 34.6
	10	7, 10, 14	9.3, 12.4, 17.4

Table 7: Bearing Capacity Based on Drained Failure as a Group Below Soil Matrix

MATRIX SOIL FRICTION ANGLE, ϕ_s (degrees)	FOOTING WIDTH (ft)	GEOPIER SHAFT LENGTH (ft)	ALLOWABLE FOOTING BEARING PRESSURE (ksf)
20 (clay)	6	7, 10, 14	6.4, 9.2, 13.7
	10	7, 10, 14	4.3, 5.7, 8.0
25 (clay)	6	7, 10, 14	11.7, 16.8, 25.2
	10	7, 10, 14	8.2, 11.0, 15.3
27 (silt)	6	7, 10, 14	15.0, 21.7, 32.4
	10	7, 10, 14	10.7, 14.3, 19.9
30 (sandy silt, silty sand)	6	7, 10, 14	22.0, 31.6, 47.2
	10	7, 10, 14	15.8, 21.2, 29.6

REFERENCES

Aboshi H., E. Ichimoto, K. Harada, M. Emoki, 1979, "The Compozer: A Method to Improve Characteristics of Soft Clays by Inclusion of Large Diameter Sand Columns," Colloque Inter. Sur le Reinforcement des Sols, ENPC-LCPC, 211-216, Paris.

Bowles, J.E., 1988, Foundation Analysis and Design, 4th Edition, McGraw-Hill, Inc., New York.

Hansen, J.B., 1970, "A Revised and Extended Formula for Bearing Capacity," Danish Geotechnical Institute Bulletin, No. 28, Copenhagen, 28 pp.

Hughes, J.M.O. and N.J. Withers, 1974, "Reinforcing Soft Cohesive Soil with Stone Columns," Ground Engineering, May, 42-49.

Meyerhof, G.G., 1976, "Bearing Capacity and Settlement of Pile Foundations," Journal of Geotechical Engineering, ASCE, vol. 102, GT3, March, pp. 195-228.

Mitchell, J.K., 1981, "Soil Improvement: State-of-the-Art Report," Session 12, Tenth International Conference on Soil Mechanics and Foundation Engineering, Stockholm, Sweden, June 15-19.

Naval Facilities Design Command (NAVFAC), 1983, Design Manual DM 7.2.

Priebe, H., 1978, "Abschaetzung des Scherwiderstandes eines durch Stopfverdichtung verbesserten Baugrundes," Die Bautechnik, (55), 8, 281-284.

ACKNOWLEDGEMENT

This Technical Bulletin was prepared by Dr. Kord J. Wissmann, P.E., President, Geopier Foundation Company, Inc. The author is indebted to Distinguished Professor Emeritus Richard L. Handy of Iowa State University and Professor George M. Filz of Virginia Tech for reviewing this technical bulletin and providing valuable insights and suggestions to the work.

Geopier Foundation Company, Inc.
150 Fairview Road, Suite 335
Mooresville, NC 28117

Telephone: (704) 799.3185 or (800) 371.7470
Fax: (704) 799.3235

e-mail: info@geopier.com
www.geopier.com

Tensar®

GEOPIER® FOUNDATIONS

Geopier Foundation Company, Inc.

800.371.7470
www.geopier.com

2_2012